BSC

Model Administrative Change Notice

Complete only applicable items.

1. Document Number:	ANL-EBS-MD-000027	2. Revision:	03	3. ACN:	03
4. Title:	Drift Degradation Analysis				
5. No. of Pages Attached	3				

6. Approvals:

Preparer:	Sounia Kassabian Darnell (Print name and sign)	7-28-06 (Date)
Checker:	Cheryl Hastings (Print name and sign)	7-28-06 (Date)
QER:	Darrell Svalstad (Print name and sign)	7-28-06 (Date)
Independent Technical Reviewer:	Robert Howard (Print name and sign)	28 July 2006 (Date)
Responsible Manager:	Mike Cline (Print name and sign)	7/28/06 (Date)

7. Affected Pages	8. Description of Change:
Page 5 of the ACN 01 form	Clarification CR-8189 identified that page 5 of Model Administrative Change Notice form for ACN 01 indicates an additional page (9-4a) was added to the document, but the specified page is not found in the final changed AMR. Page 9-4a and 9-6a were included in the draft version of the changed AMR that showed modifications using Track Changes. When the modifications were accepted in the process of finalizing the ACN, the text no longer spilled over onto an additional page and thus pages 9-4a and 9-6a were no longer generated. In finalizing the ACN, the ACN form was not updated to indicate that pages 9-4a and 9-6a were no longer generated. This clarification is related to CR-8189
6-169	Editorial Correction Figure 6-129, change the X axes label, change: Power Spectral Density in Max (H1, Vert) Time History (x 10^5) To Power Spectral Density for Vertical Component Velocity Time History (m^2/sec x 10^5) Note: There is no change to the values in the plot. This change was identified in CR-7463

1. Document Number:	ANL-EBS-MD-000027	**2. Revision**:	03	**3. ACN**:	03
4. Title:	Drift Degradation Analysis				

6-169	Editorial Correction to add clarification Figure 6-129, change the caption of the figure to add clarification, change: Rockfall Damage as a Function of the Energy Associated With the Vertical Velocity Time History. To Rockfall Damage as a Function of the Energy Associated with Vertical Component Velocity Time Histories with a Mean Annual Probability of Exceedance of 1×10^{-5} This change was identified in CR-7463
7-39	Typographical error Section **7.6.4 "Model Calibration (Confidence Building During Model Development)",** 1st paragraph on page 7-39, 4th line, change: 33º To 33.2º Note: The text is being changed to match the change in the legend in Fig. 7-21 that was made in ACN 02 This change is associated with CR-8190
7-39	Typographical error Figure 7-21 "Numerical Experiment, Category 1: Failure Envelope", on page 7-39 has been replaced to correct typographical error on the legend of the figure. Note: This change to the figure has no impact on the results of the Drift Degradation Analysis report. This change was identified previously in ACN 02 and is associated with CR-5600.
9-18	Citation update (Correct DIRS as appropriate) Reference 161949 on page 9-18, change: BSC 2002. *Software Code: UDEC*. V3.1. PC WINDOWS 2000/NT 4.0. 10173-3.1-00. 161949 To BSC 2002. *Software Code: UDEC.* V. 3.1 Sub-Release 3.10.109. WINDOWS 2000/NT 4.0. STN: 10173-3.1-00. 161949 DIRS reference has been updated by the TDMS staff

1. Document Number:	ANL-EBS-MD-000027	2. Revision:	03	3. ACN:	03
4. Title:	Drift Degradation Analysis				

9-18	Deleted reference Deleted the following reference (145366) from section 9.1: CRWMS M&O 1998. *Software Code: UNWEDGE* V2.3. V2.3. 30053 V2.3. 145366 This change was identified previously in ACN 01 and is associated with CR-4729

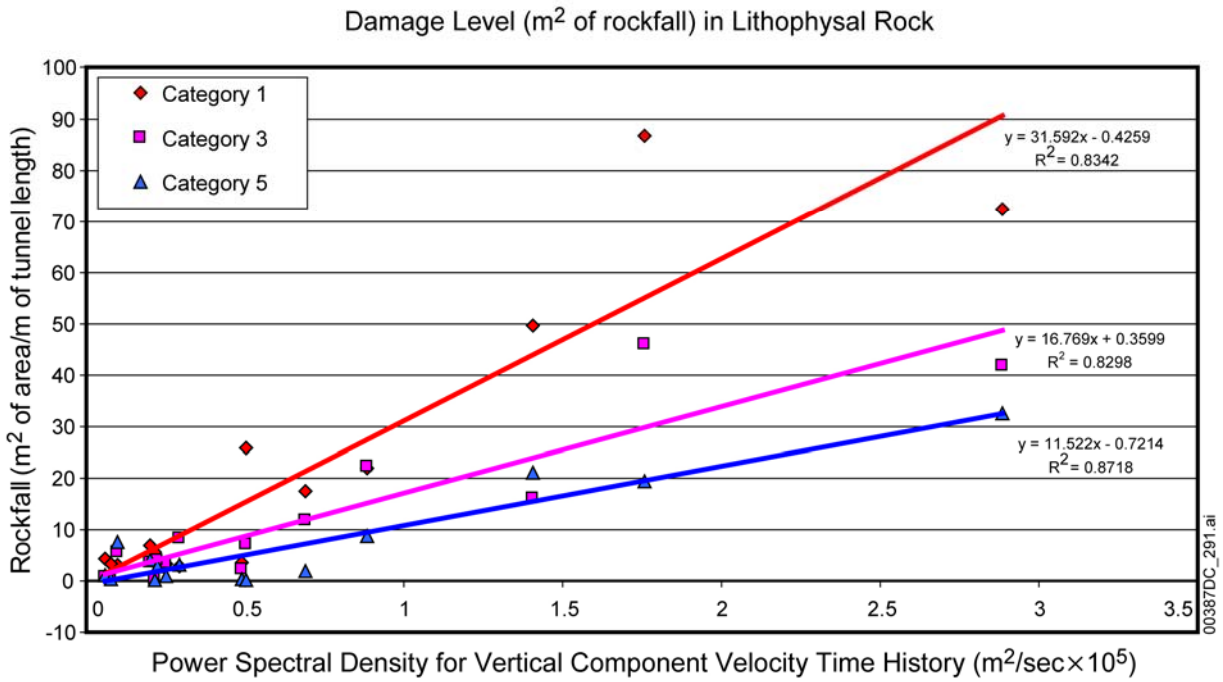

NOTE: The power spectral density is obtained by integrating the square of the velocity time history, producing a value proportional to the kinetic energy.

Figure 6-129. Rockfall Damage as a Function of the Energy Associated with Vertical Component Velocity Time Histories with a Mean Annual Probablility of Exceedance of 1×10^{-5}

Discussion–The drift damage mechanism consists primarily of shear failure at the springlines of the tunnel coinciding with passage of the compressive stress increase associated with PGV peaks in the time history. The in situ stress field has major vertical and secondary horizontal stress components. The vertical compression or horizontal shear wave essentially results in a free field dynamic stress increase as shown in Equation 6-7 (note that the correction factor of 2 in Equation 6-7 is for boundary conditions only, and therefore is not required). These dynamic components are superimposed on the existing in situ stress field to cause additional stressing or relaxation of the rock mass surrounding the drift. The end-result of this superposition is that the stress tensor rotates about the general vertical axis as the ground velocities oscillate over the duration of the strong ground motion. If the addition of dynamic plus in situ stress is large enough, shear failure occurs primarily at the springlines, resulting in development of an elliptic shape of the opening as the rock mass yields and rockfall occurs and falls along the sides of the drip shield. The extent of shear failure and rockfall around the circumference of the tunnel, up and down from the springline, is due to both the general ratio of rock mass strength to stress, but also to the ratio of the vertical to horizontal PGV. The greater the horizontal component, the greater the rotation of the stress tensor, which results in greater inclination of the major principal stress. Generally, this shear failure mechanism occurs with the arrival of the PGV peaks. Compressive stresses also appear responsible for some cases in which roof slabbing is observed where the rock mass strength and stiffness are larger (i.e., Category 5). A second failure mechanism observed includes tensile failure of the rock mass resulting from the reversal of the ground motion and inducement of dynamic tensile straining in the rock mass.

The failure envelope in the principal stress space, constructed based on numerical tests at different confinement levels, is shown in Figure 7-21. The failure envelope is curvilinear, as expected for a rock mass (similar to Hoek-Brown failure criterion). The initial friction angle (in the range of confining stress, σ_3, between 0 and 1 MPa) is 33.2°, but it decreases for larger confinement. The ratio between uniaxial compressive and tensile strengths is larger than 10.

The volumetric deformation of the model during the experiments is illustrated in Figure 7-22, which shows curves of volumetric strain versus axial strain. In general, these curves are bilinear. Initially, while the sample behaves elastically, its volume reduces due to the Poisson's effect. The initial slope of the curves is a function of the Poisson's ratio. Thus, the Poisson's ratio, ν, of the synthetic material can be calculated from the initial slope of the curve, s_e, according to the following formula derived from elasticity theory:

$$\nu = \frac{1 - s_e}{2 - s_e} \qquad \text{(Eq. 7-5)}$$

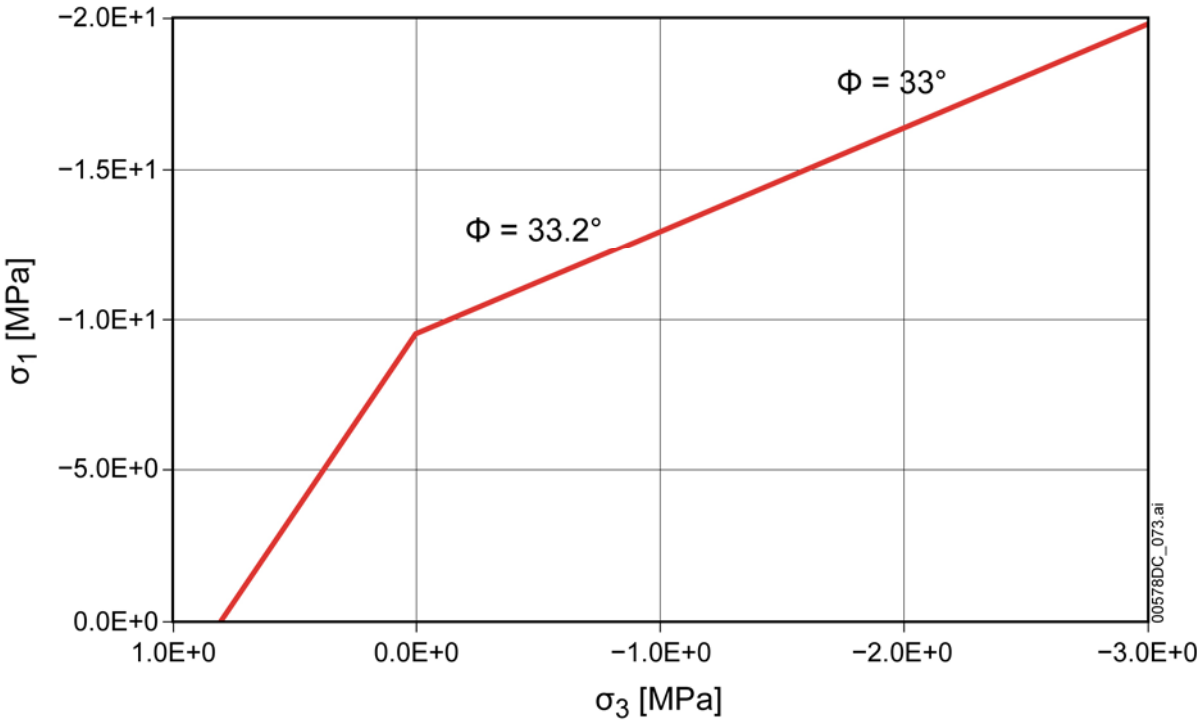

Figure 7-21. Numerical Experiment, Category 1: Failure Envelope

9.3 SOFTWARE

BSC 2002. Software Code: 3DEC. V2.01. PC WINDOWS 2000/NT 4.0. 10025-2.01-00. 161930

BSC 2002. Software Code: DRKBA. V3.31. PC WINDOWS 2000/NT 4.0. 10071-3.31-00. 161946

BSC 2002. Software Code: F LAC. V4.0. PC WINDOWS 2000/NT 4.0 10167-4.0-00. 161953

BSC 2002. Software Code: FLAC3D. V2.1. PC WINDOWS 2000/NT 4.0. 10502-2.1-00. 161947

BSC 2002. Software Code: PFC2D. V2.0. PC WINDOWS 2000/NT 4.0. 10828-2.0-00. 161950

BSC 2002. *Software Code: PFC3D*. V.2.0. PC. 10830-2.0-00. 160612

BSC 2002. *Software Code: UDEC*. V3.1 Sub-Release 3.10.109. WINDOWS 2000/NT 4.0. 10173-3.1-00. 161949

BSC 2004. *Software Code: Clustran*. V. 1.1. PC, Windows 2000. 11162-1.1-00. 169203

BSC 2004. *Software Code: PFC2D*. V 2.0. PC, Windows 2000. 10828-2.0-01. 169930

BSC 2004. *Software Code: PFC3D*. V 2.0. PC, Windows 2000. 10830-2.0-01. 169931

BSC 2004. *Software Code: Read DXF*. V. 1.0. PC, Windows 2000. 11159-1.0-00. 169204

CRWMS M&O 1997. *Software Code: DIPS*. V4.03. 30017 V4.03. 149839

Dynamic Graphics 2000. *Software Code: EARTHVISION*. 5.1. SGI/IRIX 6.5. 10174-5.1-00. 167994

LLNL (Lawrence Livermore National Laboratory) 2002. *Software Code: NUFT*. V3.0s. Sun, SunO.S. 5.6 & 5.7. 10088-3.0s-01. 157280

USGS 1999. *Software Code: FracMAN*. V.2.512. PC, Windows NT. 10114-2.511-00. 160577

9.4 SOURCE DATA, LISTED BY DATA TRACKING NUMBER

GS000608314224.004. Provisional Results: Geotechnical Data for Station 35+00 to Station 40+00, Main Drift of the ESF. Submittal date: 06/20/2000. 152573